HHS Public Access

Author manuscript

Neuroimage. Author manuscript; available in PMC 2022 November 02.

Published in final edited form as:

Neuroimage. 2022 August 15; 257: 119287. doi:10.1016/j.neuroimage.2022.119287.

Normal aging in mice is associated with a global reduction in cortical spectral power and network-specific declines in functional connectivity

Asher J. Albertson[a], **Eric C. Landsness**[a], **Michelle J. Tang**[b], **Ping Yan**[a], **Hanyang Miao**[a], **Zachary P. Rosenthal**[c], **Byungchan Kim**[d], **Joseph C. Culver**[e,f,g,h], **Adam Q Bauer**[e,f,†,*], **Jin-Moo Lee**[a,e,f,†,*]

[a]Department of Neurology, Washington University School of Medicine, 660 S. Euclid Ave, St. Louis, MO, 63110, USA

[b]Duke University School of Medicine, DUMC 3878, Durham, NC 27710, USA

[c]Medical Scientist Training Program, Washington University School of Medicine, 660 S. Euclid Ave, St. Louis, MO, 63110, USA

[d]Boston University School of Medicine, 72 East Concord St., Boston, MA 02118, USA

[e]Department of Radiology, Washington University School of Medicine, 660 S. Euclid Ave, St. Louis, MO, 63110, USA

[f]Department of Biomedical Engineering, Washington University, 1 Brookings Drive, St. Louis, MO, 63130, USA

[g]Department of Physics, Washington University, 1 Brookings Drive, St. Louis, MO 63130, USA

[h]Department of Electrical and Systems Engineering, Washington University, 1 Brookings Drive, St. Louis, MO 63130, USA

Abstract

Normal aging is associated with a variety of neurologic changes including declines in cognition, memory, and motor activity. These declines correlate with neuronal changes in synaptic structure

[*]Corresponding authors. Adam Q. Bauer: Washington University School of Medicine, Couch Research Building, 4515 McKinley Ave, St. Louis, MO 63110; 314–747–8436, aqbauer@wustl.edu (A.Q. Bauer), Jin-Moo Lee: Washington University School of Medicine, 660 S Euclid Avenue, Campus Box 8111, St. Louis, MO 63110; 314–747–1138, leejm@wustl.edu (J.-M. Lee).
[†]These authors share seniority

Declaration of Competing Interest
None to disclose

Credit authorship contribution statement
Asher J. Albertson: Conceptualization, Methodology, Investigation, Software, Formal analysis, Validation, Data curation, Writing – original draft, Project administration. **Eric C. Landsness:** Methodology, Software, Formal analysis. **Michelle J. Tang:** Investigation, Formal analysis. **Ping Yan:** Investigation, Formal analysis. **Hanyang Miao:** Software, Formal analysis, Validation. **Zachary P. Rosenthal:** Software, Conceptualization, Methodology. **Byungchan Kim:** Software, Formal analysis, Validation. **Joseph C. Culver:** Software, Resources, Supervision. **Adam Q Bauer:** Software, Resources, Supervision, Conceptualization, Funding acquisition. **Jin-Moo Lee:** Resources, Conceptualization, Supervision, Funding acquisition.

Supplementary materials
Supplementary material associated with this article can be found, in the online version, at doi:10.1016/j.neuroimage.2022.119287.

and function. Degradation of brain network activity and connectivity represents a likely mediator of age-related functional deterioration resulting from these neuronal changes. Human studies have demonstrated both general decreases in spontaneous cortical activity and disruption of cortical networks with aging. Current techniques used to study cerebral network activity are hampered either by limited spatial resolution (e.g. electroencephalography, EEG) or limited temporal resolution (e.g., functional magnetic resonance imaging, fMRI). Here we utilize mesoscale imaging of neuronal activity in *Thy1*-GCaMP6f mice to characterize neuronal network changes in aging with high spatial resolution across a wide frequency range. We show that while evoked activity is unchanged with aging, spontaneous neuronal activity decreases across a wide frequency range (0.01–4 Hz) involving all regions of the cortex. In contrast to this global reduction in cortical power, we found that aging is associated with functional connectivity (FC) deterioration of select networks including somatomotor, cingulate, and retrosplenial nodes. These changes are corroborated by reductions in homotopic FC and node degree within somatomotor and visual cortices. Finally, we found that whole-cortex delta power and delta band node degree correlate with exploratory activity in young but not aged animals. Together these data suggest that aging is associated with global declines in spontaneous cortical activity and focal deterioration of network connectivity, and that these reductions may be associated with age-related behavioral declines.

Keywords

Aging; Functional connectivity; Cortex; GCaMP

1. Introduction

Normal aging is associated with declines in cognition across many domains including executive function, memory, and language production (Salthouse, 1998; Blazer et al., 2015; Shafto et al., 2007). Aging is also associated with reductions in sensorimotor function including slower performance of visuomotor tasks (de Bruin et al., 2016), reduced walk speed (Bohannon, 1997), declines in motor planning and dexterity (Stockel et al., 2017), and worsened coordinated movement (Serrien et al., 2000). These functional declines happen in concert with significant cerebral changes. Brain weight (Terry et al., 1987), myelinated fibers (Marner et al., 2003), and cortical thickness (Salat et al., 2004) all decline in relatively linear fashion during normal aging. Interestingly, these changes are not correlated with significant neuronal loss, but are rather associated with synaptic changes (Morrison and Baxter, 2012). Multiple studies in primate and rodent models have demonstrated age-related changes in dendritic length (Dickstein et al., 2013), spine number and type (Dickstein et al., 2013), synaptic dynamics (Mostany et al., 2013), as well as short (Ou et al., 1997) and long term synaptic plasticity (Shankar et al., 1998). White matter tracts also decline with age. Fiber tractography reveals that white matter tract integrity peaks in midlife before gradually diminishing with age (Yeatman et al., 2014; Hasan et al., 2009; Zhao et al., 2015).

The mechanisms by which the observed synaptic, neuronal, and white matter tract changes seen with aging lead to functional declines in behavior are poorly understood. One likely consequence of age-associated synaptic changes is disruption of neuronal network activity. Deterioration of large-scale cortical networks with aging may bridge the cellular and

molecular changes of aging with the behavioral decline observed in aging. Network level synchronous brain activity is hypothesized to coordinate information transfer and contribute to sensory and cognitive functions (Giraud and Poeppel, 2012; Ward, 2003). Previous human studies have shown that aging is associated with significant changes to brain spontaneous activity and these changes may be indicators of cognitive performance (Klimesch, 1999). Perhaps most compelling, normal aging is associated with a significant and linear decline in resting state spontaneous cerebral activity in slower frequency ranges (0.5–6.5 Hz) and slow wave power in older individuals is a significant predictor of cognitive performance (Vlahou et al., 2014).

Functional connectivity across brain networks may offer another important link between age-related synaptic changes and behavioral declines. fMRI-based resting state functional connectivity (FC) studies have demonstrated significant effects of aging on network connectivity (reviewed by Damoiseaux JS (Damoiseaux, 2017)). Among other changes, aging is significantly associated with decreased connectivity in both the anterior and posterior components of the default mode network (Wu et al., 2011). Grady et al. further demonstrated reduced connectivity in the default mode network as well as increased inter-network connections for the frontoparietal control and dorsal attention networks in aged individuals during tasks (Grady et al., 2016). These and other studies strongly suggest that normal aging is associated with regional reorganization of network functional connectivity. Additionally, age related changes in FC have been shown to correlate with behavioral and cognitive changes in several domains. These include age-related changes in somatomotor integration (Yoshimura et al., 2020), motor learning (Mary et al., 2017), and memory (Sala-Llonch et al., 2014).

Prior studies of cortical network activity and connectivity have typically utilized either EEG or fMRI. While EEG studies have relatively high temporal resolution, they have significantly limited spatial resolution (Burle et al., 2015). The EEG signal is limited by nature in recording brain-derived field potentials through scalp and skull tissue which acts to smooth the recording and limit spatial resolution (Srinivasan et al., 1996). This limitation is further exacerbated by variability in head size, skull thickness, tissue type, and body temperature (McCann et al., 2019). Conversely, fMRI offers better spatial resolution, but has limited temporal range with observations restricted to activity in the infraslow spectra (< 0.08 Hz) (Anderson, 2008). Furthermore, the BOLD signal measured in fMRI studies represents a vascular, indirect measure of neuronal activity (Logothetis and Wandell, 2004). This is an important confound because numerous studies have demonstrated age-related deteriorations in neurovascular coupling (Fabiani et al., 2014; Park et al., 2007).

Here, we seek to address these limitations by characterizing age-related changes in the cortical network activity and connectivity by performing direct mesoscale (whole cortex) imaging of neuronal network activity in young and aged *Thy1*-GCaMP6f transgenic mice. Projection neurons within these mice produce a robust fluorescent signal with fast activation and deactivation and high signal to noise ratio in association with suprathreshold neuronal activity (Chen et al., 2012; Dana et al., 2014; Xiao et al., 2017). Use of this technique allows direct characterization of age-related neuronal network changes with high temporal and spatial resolution (Brier et al., 2019; Wright et al., 2017). We chose

to examine cortical networks via several measures including evoked and spontaneous activity. We examined network connectivity using seed-based and homotopic correlations as well as whole-cortex node degree. While we first observed a global decline in cortical spectral power, our observations of functional connectivity revealed a significant visual and somatomotor component, so we quantified spontaneous behavior in aged and young animals and correlated these levels to whole-cortex spontaneous activity and network connectivity.

2. Methods

2.1. Animals

A total of 33 transgenic *Thy1*-GCaMP6f mice (Jackson Laboratories C57BL/6J-Tg (Thy1-GCaMP6f)GP5.5Dkim/J; Stock Number 024,276) were used in this study. 16 (7 female and 9 male) young mice aged (2–3 months) and 17 (8 female and 9 male) aged mice (17–18 months) were included in the study. Ages were chosen as representative correlates for early adulthood (approximately 20 years old) and older age (approximately 60 years) (Fox, 2007). Healthy aging is associated with some motor (Studenski et al., 2011) and cognitive declines (Salthouse, 1998) in the 7th decade of life, so mice correlating to this age were chosen for the aged group. Mice were housed in standard cages with ad libitum access to food and water in a dedicated animal facility under a 12 hour light/12 hour dark cycle. All experimental protocols were approved by the Animal Studies Committee at Washington University and all studies were conducted in accordance with the US Public Health Service's Policy on Humane Care and Use of laboratory animals.

2.2. Extracranial window placement

Mice were anesthetized with inhalation isoflurane (4.0% induction, 1.5% maintenance) and placed into a stereotaxic head fixation frame (Kopf Instruments, Tujunga, CA, USA). Each mouse was placed on a heating pad and temperature was maintained at 37 °C via feedback from a rectal probe (mTCII Cell Microcontrols, Norfolk, VA, USA). The head was thoroughly shaved and cleaned and a midline incision was performed as previously described (Brier et al., 2019; Wright et al., 2017; Rosenthal et al., 2020). The scalp was retracted, and a custom-made clear Plexiglas window was affixed directly to the skull using dental cement (C & B Metabond, Parkell, Edgewood, NY, USA). Mice were monitored daily after window placement.

2.3. Imaging acquisition

GCaMP calcium imaging was performed as previously described[29]. Mice were placed in a felt pouch and their heads secured via small screws in the plexiglass windows under an overhead cooled, frame-transfer EMCCD camera (iXon 897, Andor Technologies, Belfast, Northern Ireland, United Kingdom) with an approximately 1cm^2 field of view covering the entire dorsal view of the cortex. Sequential illumination was provided by four LEDs: a 470 nm LED used for GCaMP6f excitation (measured peak λ=454 nm), while 530 nm (measured peak λ=523 nm), 590 nm (measured peak λ=595 nm) and 625 nm (measured peak λ=640 nm) LEDs were used for optical intrinsic signal imaging (described below). All LEDs were purchased from Mightex Systems, Pleasanton California, USA. For each LED, the duration of illumination was as follows: 20 ms (454 nm), 5 ms (523 nm), 3 ms (595 nm),

and 1 ms (640 nm). The 454ngm and 523 nm LED light paths were made collinear by using a multiwavelength beam combiner dichroic mirror (LCS-BC25–0505, Mightex Systems). An 85 mm *f*/1.4 camera lens (Rokinon, New York, New York, USA) collected all reflected light. The overall camera framerate was approximately 67 Hz, resulting in an acquisition frame rate of 16.81 Hz per channel. As previously described, this framerate is fast enough to capture GCaMP6f activity (Wright et al., 2017). Full frame images (512 × 512 pixels) were binned (4 × 4 pixels) on camera to increase SNR providing a final image resolution of 128 × 128 pixels. The LED and the CCD were synchronized and triggered via data acquisition card (PCI-6733, National Instruments, Austin, TX, USA) using custom written MATLAB scripts (MathWorks, Natick, MA, USA). The field-of-view was adjusted to cover the entire visible cerebral cortex with a total area of approximately one square centimeter and each pixel representing approximately 78 × 78 micrometers. Linear polarizers were used in front of the of the LED sources and CCD lens to minimize specular reflectance from the skull. Data from all imaging sessions were acquired and stored in 5-minute intervals. Fifteen minutes of resting state imaging and 10 min of imaging during forepaw stimulation were collected in each mouse.

For awake, resting state imaging, mice were acclimatized to the imaging felt pouch for several minutes and allowed to move freely with the exception of their restrained head. The room was kept dark and imaging was only commenced when mice were resting comfortably. This was defined as no observable movement in the neck or head, lack of attempt to free themselves from the frame, and/or resumption of typical murine behavior including whisking (similar to our prior work (Rosenthal et al., 2020)). For stimulus induced imaging, mice were anesthetized with an intraperitoneal injection of ketamine/xylazine (86.9 mg/kg ketamine, 13.4 mg/kg xylazine). After anesthesia, the animals were placed on heating pads maintained at 37 °C as described above. Transcutaneous forepaw stimulation was performed similar to prior studies (Kraft et al., 2018) via placement of microvascular clips (Roboz Srugical Equipment, Gaithersburg, MD, USA) on the right wrist. Electrical stimulation was via a block design (0.5 mA, 3hz stimulation, 5 s, 30 events in 5 min).

2.4. Image processing

All data was subjected to an initial quality check and all data with movement contamination were excluded. Image processing was as previously described (Wright et al., 2017; Kraft et al., 2018; White et al., 2011). A binary brain mask was created and applied by tracing the field of view to include only the brain component using the roipoly.m function in Matlab. Image sequences from each mouse were affine-transformed to a common atlas space (based on the Paxinos mouse atlas) using the positions of bregma and lambda. Images were smoothed with a 5 × 5 Gaussian filter. Baseline/ambient light levels were subtracted from the raw data. All pixel time traces were spatially and temporally detrended to correct for variations in light levels. Fluorescence emission during the 454 nm LED illumination were used to analyze the GCaMP signal and a ratiometric correction for absorption by hemoglobin and deoxyhemoglobin was used as previously described (Wright et al., 2017) and as outlined in summary below.

The 523 nm LED was used as an emission refence for the GCaMP6f fluorescence to remove any confound from the hemodynamic signal in the fluorescent signal. The fluorescence and 523 nm reflectance data were mean normalized and the ratio of the fluorescent emission data divided by the 523 nm reflectance data was used to correct the fluorescence data for the absorption dynamics due to oxyhemoglobin and deoxyhemoglobin changes. The modified Beer-Lambert's law was solved using the 523, 595, and 640 nm wavelength reflected intensities to identify oxy and deoxy hemoglobin changes.

The time traces for all pixels within the brain mask were averaged to create a global cortical signal. For all resting state and activation analysis, this global signal was regressed from every pixel's time trace to remove global sources of variance. Resting state data was filtered into canonical frequency ranges of 0.01–0.2 Hz (Infraslow) and 1–4 Hz (Delta). Power spectral analysis was computed using a Hann window and fast Fourier transform. The square moduli of these FFTs were then averaged across the cortex to produce the final power spectra.

Seed-based functional connectivity was calculated by placing seeds (0.25 mm diameter containing approximately 30 pixels) in each hemisphere (16 total seeds). Seeds were placed at canonical locations expected to correspond with the bilateral frontal, motor, somatosensory, parietal, cingulate, retrosplenial, auditory, and visual cortices. Seed locations were determined prior to imaging using an anatomic atlas (Franklin and Paxinos, 2013) similar to our prior work (White et al., 2011; Bauer et al., 2014; Bero et al., 2012). For each seed region, time traces of GCaMP fluorescence were correlated with time courses in all brain pixels generating an FC map for each seed. Individual mouse maps were transformed into Fisher z-scores and averaged within each group (aged and young). Homotopic functional connectivity was calculated by correlating the time trace of each pixel in the left hemisphere to the time trace of its contralateral homolog. Correlation values underwent Fisher z-transformation and were averaged on a group level. Node degree was calculated by determining the number of pixels (degree) with which a particular pixel (node) had a correlation above threshold ($r \geq 0.4$) similar to prior work (Hakon et al., 2018).

2.5. Histology and microscopy

Mice were deeply anesthetized with FatalPlus (Vortech Pharmaceuticals, Dearborn, MI, USA) and transcardially perfused with 0.01 mol/L, ice cold, heparinized, Phosphate Buffered Saline (PBS). The brains were removed and submerged in 4% paraformaldehyde for 24 h. Brains were then transferred to a solution of 30% sucrose in PBS Brains were sliced at 50 μM thickness on a sliding microtome (Microm, Boise, ID, USA). Sections were stored in 0.2 M PBS, 20% Sucrose, and 30% ethylene glycol at −20 °C. For cell counting, 3 mice from each group (aged and young) were utilized and 3 sections (as above) from each mouse were imaged. Imaging of GCaMP6f expression was performed using an inverted confocal microscope (Nikon A1-Rsi). 4 fields were identified in each section (layer 2/3 barrel cortex, layer 5 barrel cortex, layer 2/3 motor cortex, and layer 5 motor cortex) and 1 image was taken from each field (9 total images from each field). Images were acquired as *z*-stacks through the thickness of the section (1 μm step distance). Images were exported

and compiled into maximum intensity projections (ImageJ) and fluorescent (GCaMP+) cells were counted manually.

2.6. Evaluating spontaneous behavior

Spontaneous mouse activity was observed by placing the mice in a clean, clear container and recording their spontaneous behavior for 5 min. Cameras (Kodak, Rochester, NY, USA) were placed immediately adjacent to the cylinder with a side view and recorded for 5 min (60FPS). Videos were exported and analyzed using custom-written scoring software on a frame-by-frame basis. We divided spontaneous mouse activity into 3 categories for simpler quantification. Wall exploration was quantified as the number of frames the animals was touching the walls of the container normalized to the total number of frames. Self-grooming behavior was defined as rubbing paws, licking, scratching, and running paws through hair normalized to total number of frames. Immobility was defined as the number of frames not moving normalized to the total number of frames.

2.7. Statistics

All statistical analyses were performed using either Matlab or Prism Graphpad Software. For evoked responses, an ROI was drawn around the area of somatosensory activation (defined by all the pixels with activation amplitudes during forepaw stimulation within the 75% of the maximum activation). Within this ROI, we calculated the average intensity in aged and young animals. Additionally, we calculated total area of activation between aged and young animals by counting the number of pixels within the defined 75th percentile of the maximum activation. Statistically significant differences in whole-cortex power, node degree, and homotopic functional connectivity were calculated by comparing young and aged mice with unpaired, two sample *t* tests.

Analysis of power and FC carries a high risk of Type 1 error due multiple comparisons across the large number of pixels and the risk of Type 2 error when applying a classic correction such as the Bonferroni across the mask. We used a cluster-based, non-parametric, permutation method described by Maris and Oostenvel (Maris and Oostenveld, 2007), which groups pixels into clusters based on data variance across conditions, thus minimizing the number of multiple comparisons and optimizing both Type 1 and Type 2 errors. The test statistics were *t* test statistics for z(R), power, and node degree. Briefly, pixels with test statistics less than p value 0.05 threshold were clustered into continuous areas, from which the cluster statistics were calculated by the summation of the test statistics of the pixels in each cluster. A null hypothesis distribution of cluster statistics was obtained by iterating 2000 times a random assignment of data to different conditions, calculating the test statistics of each pixel, and obtaining the cluster statistics. Clusters were determined to be statistically significant if they were greater than 97.5 percent of the null hypothesis cluster statistic distribution with n degrees of freedom (where n = total subject/2). Difference maps were generated for and thresholded to significance for power, homotopic FC, and node degree.

Seed based functional connectivity matrices were compared via an unpaired Student’s t-test with a false discovery rate (FDR) correction. Behavioral correlations were performed by plotting exploration against node degree or power (delta or infraslow) within a region of

interest drawn around the cortical space which showed significant aged-related differences and performing simple linear regression to calculate an R squared value. Correlations were tested for non-linearity via an F test and a p value of less than 0.05 was considered significant.

3. Results

3.1. GCaMP neuron density and somatosensory-evoked activation are similar between young and aged mice

We compared cellular and physiologic characteristics of *Thy1*-GCaMP6f mice at two different ages: Young mice (2 to 3 months) and aged mice (17 to 18 months). To ensure that differences between ages were not due to changes in the density of GCaMP-expressing neurons, we first quantified GCaMP expressing cells within the cortex of young ($n = 3$) and aged animals ($n = 3$) in primary motor cortex (M1) and barrel cortex (S1Bf) (Fig. 1a & Fig. 1b). We found no age-dependent differences in GCaMP positive cell density in layer 2/3 barrel (Young = 55.86 ± 4.36 cells/mm^3; Aged = 54.12 ± 4.86 cells/mm^3) and primary motor cortex (Young = 49.75 ± 1.51 cells/mm^3; Aged = 55.86 ± 8.32 cells/mm^3) or in layer 5 in barrel (Young = 193.77 ± 11.41 cells/mm^3; Aged = 173.70 ± 6.1 cells/mm^3) and primary motor cortex (Young = 160.61 ± 3.15 cells/mm^3; Aged = 147.51 ± 10.72 cells/mm^3) (Fig. 1c). To determine if differences between ages were due to changes in GCaMP activation, we next examined sensory-evoked activity. Somatosensory cortex activity was evoked via mild electrical stimulation of the right forepaw (Fig. 2a). Stimulation evoked robust local somatosensory cortex activation in both young and aged mice (Fig. 2b). Stimulation intensity was similar to prior experiments which demonstrated consistent, reproducible forepaw somatosensory cortex activation (Kraft et al., 2018). We quantified somatosensory activation intensity by drawing an ROI around the region of activation (defined by all the pixels with activation amplitudes during forepaw stimulation within the 75% of the maximum activation) and calculating the average intensity in aged and young animals. We also calculated total area of activation between aged and young animals by counting the number of pixels within the defined 75th percentile of the maximum activation. We found no significant difference in either intensity (%ΔF/F) (Young = 0.23 ± 0.081; Aged = 0.27 ± 0.076) or area of activation (measured as pixels above threshold) (Young = 2143.7 ± 17.22; Aged = 153.4 ± 22.63) in aged vs. young mice (Fig. 2c). Averaged traces of GCaMP signal intensity in the aged vs young cortex are shown in (Fig. 2d). These data indicate that neither the density of GCaMP expressing neurons nor evoked GCaMP activity changed with aging.

3.2. Cortical resting state power is globally reduced across all frequencies with aging

Compared to neural activity, hemodynamic measures of brain activity (e.g. fMRI, OISI) are relatively slow (the hemodynamic response function primarily acts as a low pass filter). Further, a variety of non-neurologic factors, including changes in neurovascular coupling and changes in vasoreactivity (Reviewed by Lu et al. (Lu et al., 2019)), limit interpreting how local changes in neuronal activity relate to subsequent hemodynamics. We therefore sought to characterize spontaneous neuronal network activity using the high temporal and spatial resolution provided by GCaMP imaging. We examined band-limited power over the

entire cortex across a wide range of frequencies (0.01 Hz–4 Hz). Global spontaneous neural fluctuations in aged mice were generally lower across the entire frequency range (Fig. 3a). To quantify frequency-specific changes in neural activity, we subdivided activity into bins of equal relative bandwidth (2 octaves/bin) (Fig. 3b). Aging was associated with a significant reduction in spontaneous neuronal activity across each of these bins (0.02–0.08 Hz, $p = 0.03\times10^{-4}$; 0.04–0.16 Hz, $p = 0.03\times10^{-4}$; 0.08–0.32 Hz, $p = 0.17\times10^{-4}$; 0.16–0.64 Hz, $p = 0.12\times10^{-4}$; 0.32–1.28 Hz, $p = 0.75\times10^{-4}$; 0.64–2.56 Hz, $p = 0.895\times10^{-4}$; 2.56–4.0 Hz, $p = 0.035$).

We next examined whether the reductions in resting state activity were focal or global. Two canonical frequency ranges were examined, delta (1–4 Hz) and infraslow (0.01–0.2 Hz). Maps of average power in young (top row) and aged (middle row) in both the delta (Fig. 3c) and infraslow (Fig. 3d) bands are shown. Within both frequency bands, we see the greatest power in the motor, parietal and somatosensory cortices similar to prior observations (Brier et al., 2019). We then created difference maps between young and aged animals (young minus aged) thresholded for significance. We found a significant reduction in resting state activity in the delta and infraslow frequency bands throughout most of the cortex (Fig. 3c and Fig. 3d).

3.3. Functional connectivity reductions are network specific in aged mice

Given the broad decline of spontaneous activity, we next examined the effect of aging on network connectivity. 8 canonical “seeds”, representing previously defined network nodes (as described in Methods), were placed on each side of the brain at the mid-point of unique networks (left and right frontal, motor, somatosensory, parietal, cingulate, retrosplenial, auditory, and visual). Group average maps of the connectivity of the entire cortex to the seed networks in the delta (Fig. 4a) and infraslow (Fig. 4b) frequency bands in young and aged (Fig. $4A_1$ and B_1) animals were generated. Correlation matrices (White et al., 2011; Hakon et al., 2018) were generated in young and aged mice (Fig. $4A_2$ and $4B_2$), and difference matrices were calculated (young minus aged) (bottom row Fig. $4A_2$ and $4B_2$). We found that aging was associated with significant deterioration of connectivity between select networks. Most notably, connectivity between parietal and motor and cingulate and motor seeds were significantly different with age across both the infraslow and delta frequency bands. Differences were also observed in retrosplenial and somatosensory seeds. We did not observe connectivity differences within the visual or frontal seeds.

Because a large proportion of the FC changes we observed were interhemispheric, we next compared homotopic FC in aged and young mice by measuring the correlation of each pixel on one side of the brain to its contralateral homologue. As this FC measure is symmetric about midline, homotopic FC is visualized in the left hemisphere while network assignments (based on the Paxinos atlas) are visualized in the right hemisphere. Consistent with prior work (Hakon et al., 2018), stronger homotopic FC was observed in motor, somatosensory, and visual cortices in both the delta frequency (Fig. 5a) and infraslow frequency bands (Fig. 5b). Age-related homotopic FC changes were strikingly focal in comparison to the global power changes. Aged mice showed significantly less homotopic functional connectivity

in the motor (delta and infraslow bands) and somatosensory (infraslow band) and visual (infraslow band) cortices.

Another salient observation in the seed-based FC maps of Fig. 3 was a global trend towards reduced positive correlation in aged mice. We quantified this decline in FC by calculating the total number of functional connections (node degree) of each pixel across the entire cortex in the delta (Fig. 6a) and infraslow (Fig. 6b) frequency bands. We found robust cortical node degree in both frequency bands in the motor, somatosensory, and visual cortices. We found more wide-spread age-related loss of node degree in the infraslow frequencies than the delta frequency band. Within the delta frequency band, aging was associated with significant reduction of motor cortex node degree. Within the Infraslow band, aging was associated with significant reduction of somatosensory, and visual cortex node degree. In addition to pixel by pixel analysis of node degree across the entire cortex (Fig. 6) we also examined average node degree within the seeds used for seed-based FC analysis and compared them across young and aged animals (Fig. 7). This again demonstrated widespread loss of node degree with aging (more predominant in the infraslow band) particularly in motor, somatosensory, and visual cortices.

In contrast to our observation of a relatively global decrease in resting state power within the aged cohort, we observed more network specific changes in functional connectivity with aging (Summarized in Fig. 7). Age-associated deterioration of node degree (sphere size) was more predominant in the infraslow band and demonstrated significant reductions in the bilateral visual and parietal cortices as well as smaller reductions in unilateral frontal, cingulate, retrosplenial, and auditory cortices. Seed-based deterioration of FC (red and blue lines) in aged animals as noted in Fig. 4 was observed in several networks including sensory, motor, and cingulate networks. Notably, the majority of aged-associated FC deterioration was between negatively correlated regions (blue vs red lines).

3.4. Global power and node degree correlate with activity in young but not aged mice

Physical Activity levels in mice (Lamberty and Gower, 1992) and humans (Milanovic et al., 2013) decline with age. Given the sensorimotor predominance of the observed connectivity differences between young and aged animals, and the previously reported declines in overall activity in mice and humans with age, we chose to examine the behavior of mice exploring a clear cylinder- a well-established test of sensorimotor function (Schallert et al., 2000). To compare spontaneous mouse behavior between young and aged groups, we scored time spent on: wall exploration (Fig. $8a_1$), self-grooming (Fig. $8a_2$), and inactivity (Fig. $8a_3$). We observed significantly less wall exploration time in aged mice (% frames exploring) (Young = 4.93 ± 0.53, $n = 17$; Aged=2.57 ± 0.43, $n = 18$; $p = 0.0014$) and significantly more inactive time (% frames inactive) (Young = 12.91 ± 2.51, $n = 17$; Aged=24.83 ± 2.96, $n = 18$; $p = 0.0044$). We did not find a significant difference in grooming behavior between young and aged mice (% frames grooming) (Young = 5.20 ± 0.67, $n = 17$; Aged=7.94 ± 1.38, $n = 18$; $p = 0.088$).

We examined the correlation between whole-cortex power in the delta and infraslow spectrum and wall exploration on an individual mouse level. Differences in n value between total mice undergoing behavior analysis and mice undergoing correlation analysis are due to

exclusion of mice with significant imaging artifact prior to correlation analysis. We found that young (n = 14) mice exhibited a significant correlation between wall exploration and whole-cortex, resting-state delta power (Fig. 8b$_1$) (R^2 = 0.46; p = 0.008). Wall exploration did not correlate with infralow power (Fig. 8b$_1$) (R^2 = 0.0.016; p = 0.67). We further did not observe a correlation between inactivity and power. Aged mice (n = 11), which were significantly more immobile overall, did not exhibit this correlation (Fig. 8b$_2$) (R^2 = 0.19; p = 0.17). We next examined whether whole-cortex node degree correlated to mouse activity. We found that average whole-cortex node degree correlated (R^2 = 0.33; p = 0.046) with wall exploration in young mice (n = 13) (Fig. 8b$_3$), but not aged mice (n = 9) (Fig. 8b$_4$). As with resting state power, this correlation was noted only in the delta band.

To determine if specific networks were responsible for the correlation between whole-cortex power/node degree and exploratory behavior, we examined the correlation between exploratory behavior and average resting state power and average node degree within different networks (as outlined in Fig. 5). Delta power within the somatomotor (R^2 = 0.3; p = 0.042), visual (R^2 = 0.33; p = 0.032), and retrosplenial networks (R^2 = 0.43; p = 0.012) correlated significantly with exploratory activity in young but not aged animals (Supplemental Figure 1). Moreover, Delta band node degree within the somatomotor (R^2 = 0.32; p = 0.04), and visual cortex (R^2 = 0.33; p = 0.04), correlated significantly with behavior in young but not aged animals. Infraslow band power and node degree did not correlate with behavior (Supplemental Figure 2).

4. Discussion

4.1. General findings

We utilized mesoscale imaging in *Thy1*-GCaMP6f mice to directly compare spontaneous neural activity and network connectivity in aged and young animals with high spatiotemporal resolution. Aging was associated with a nearly global decrease in spontaneous network activity across the spectrum of frequencies we examined (0.01–4 Hz). This decrease in resting state power was present throughout most of the cortex. In contrast to the widespread changes in resting state neuronal activity, we observed that aging was associated with more focal changes in functional connectivity. In examining homotopic FC, seed-based FC, and global node degree, aged animals exhibited reduced FC in several cortical regions including motor, parietal, and visual cortices. Examination of spontaneous behaviors revealed that exploratory activity in young mice significantly correlated with whole-cortex resting state delta power, but not infraslow power. Aged mice, which were significantly less active, no longer exhibited this correlation. Finally, we observed that whole-cortex node degree correlated with exploratory activity in young animals. As with power, this was not observed in the infralsow frequency band and aged mice no longer demonstrated this correlation. Together these data suggest that aging is associated with broad declines in global power as well as local deterioration of connectivity within select cortical networks. These declines correlated with behavioral changes seen in aged mice and may suggest a link between the neuronal and synaptic changes observed in older individuals and behavioral declines associated with aging.

The synchronous activity of networks has been described as a “middle ground” between single neuron activity and behavior (Buzsaki and Draguhn, 2004). Spontaneous neuronal activity across a variety of frequencies has been implicated in a wide range of functions including information transfer, plasticity, memory, attention, and consciousness (Giraud and Poeppel, 2012; Ward, 2003; Cebolla and Cheron, 2019). Importantly, phase synchronization of activity in distinct brain regions is thought to underlie functional connectivity critical for the integration of information (Varela et al., 2001). Our data show two primary findings with aging: 1) a nearly global decline in resting state activity across a wide frequency range (0.01–4 Hz) that extends over much of the cortex (encompassing most of somatosensory, motor, and visual cortices), and 2) more nuanced decline in regional functional connectivity within and across resting state networks (as illustrated in Fig. 7).

4.2. Age-Associated global reduction in cortical spontaneous activity

Prior work has shown that aging is associated with significant changes to cortical spontaneous activity. Most relevant is recent magnetoencephalographic work demonstrating widespread linear declines in slow wave EEG power (0.5 – 6.5 Hz) with aging (Vlahou et al., 2014). Compellingly, this work also demonstrated that enhanced delta and theta power was associated with better performance on tests of executive function. Our work adds to the finding that aging is associated a broad decline in spontaneous activity across a wide frequency range including infraslow and delta (0.01–4 Hz) and that this decline covers most of the cortex. Additionally, we found that whole-cortex delta activity positively correlated with exploratory activity in young animals, but in aged animals (which explored significantly less and had significantly less infraslow and delta power overall), this correlation was no longer observed. Correlations between delta band power and node degree and exploratory behavior suggests a frequency specific role in some spontaneous behaviors which is lost in aged animals who exhibit significantly less exploratory behavior overall.

4.3. Age-Associated deterioration of functionally connected networks

Observations of age-associated white matter deterioration led to the “disconnection” hypothesis that cognitive decline during normal aging results from changes in the integration of cerebral networks (O’Sullivan et al., 2001). A number of functional imaging studies have since shown that aging is associated with a wide range of network and FC changes (Varangis et al., 2019; Grady, 2012). Seminal work by Andrews-Hanna et al. demonstrated that aged individuals, free from Alzheimer’s disease pathology, had significantly reduced anterior to posterior functional connectivity within the default mode network (Andrews-Hanna et al., 2007). Others have further demonstrated that aged individuals have reduced frontoparietal control and default mode network connectivity (Avelar-Pereira et al., 2017), reduced connectivity within the frontoparietal network (Campbell et al., 2012), and reduced cortico-striatal network FC (Bo et al., 2014). A recent study using fMRI in mice found an inverse U shape of functional connectivity strength in the sensory motor and default mode networks across the lifespan of mice with connectivity increasing until middle age then declining significantly (Egimendia et al., 2019). Here we leverage the high spatial resolution and broad temporal range of mesoscale calcium imaging to show that neural activity in aged mice is globally reduced. We also show that aging in mice is associated with degradation of functional connectivity in discrete cortical networks particularly somatomotor and visual

networks. Finally- we show that band specific correlations in power and connectivity with behavior in young, but not aged mice.

Many of the reductions in FC we observed in our seed-based analysis were loss of anti-correlation (summarized by the blue lines in Fig. 7a and Fig. 7b). This resulted in less discrete network borders (as seen in Fig. $4A_1$ and $4B_1$). Decreased functional specialization and network integrity has been well described with aging. Hippocampal place cells firing become less specific as animals age (Barnes et al., 1983). Older individuals utilize a greater cortical area to process visual information (Grady et al., 1994), utilize significantly less cortical specialization when viewing distinct categories of visual stimuli (Park et al., 2004), and recruit additional cerebral area during verbal memory encoding (Logan et al., 2002). Additionally, resting state FC analysis has shown decreased segregation of functional brain systems in aged individuals-particularly those older than 50 (Chan et al., 2014). The diminished anticorrelation and degradation of distinct network borders observed in our study may represent network desegregation with aging in mice. Anticorrelation between networks is thought to be an important component of attention demanding tasks (Fox et al., 2005) and, of note, human studies have also demonstrated that anticorrelation between the dorsal attention and default mode networks is attenuated in older adults (Spreng et al., 2016).

It should be noted that overall, we observed a greater dynamic range in connectivity values within the infraslow frequency band relative to the delta frequency band. This may reflect greater overall coherence of slow waves. The greater dynamic range at slow frequencies may make analysis at these lower frequencies overall more sensitive to changes across groups. This may further contribute to the broader changes seen in node degree and homotopic functional connectivity between aged and young animals (Figs. 5, 6,&7) within the infraslow band when compared to the delta band.

4.4. Correlation of delta activity and connectivity with behavior

Recent work demonstrating that delta and infraslow activity likely represent unique neural processes with separate propagation patterns (Mitra et al., 2018) supports our finding. If activity within these frequencies represent unique processing- then it is interesting to consider that while aging appears to universally drive down cortical network activity, its effect on delta activity may disproportionately affect certain somatomotor functions. Delta activity predominates cortical function during development (Scher, 2008) and slow wave sleep (Dijk, 2009). Relevant to our finding that delta activity correlates with exploratory activity, it has been highly implicated in motivational behavior (Knyazev, 2012; Knyazev, 2007). Declines in delta activity with aging may therefore underlie diminished drive to explore a new environment. Delta activity has also been associated with visual attention (Lakatos et al., 2008), hunger (Hoffman and Polich, 1998; Savory and Kostal, 2006), and reward craving (Reid et al., 2003), processes to which exploratory behavior would seem closely related. Further delineating possible frequency specific correlations with other behaviors will be an important subject of future work.

Our observation that delta frequency power and node degree correlate to exploratory behavior in young but not aged mice (which exhibit significantly less delta power and exploratory behavior overall) adds to the hypothesis that network dysfunction contributes

to age related functional decline. Prior human studies have shown a strong correlation between network behavior and behavioral declines. The majority of this work has focused on age-associated cognitive decline. Default mode network functional connectivity in older adults free of Alzheimer's pathology has a linear correlation with composite scores of executive function, memory recall, and processing speed (Andrews-Hanna et al., 2007). Memory decline itself is conversely correlated with default mode network FC (Bernard et al., 2015). Decreased FC within the salience network is noted with aging and the degree of impairment correlates with decreased scores on a battery of cognitive neuropsychiatric tests (Onoda et al., 2012). Innovative work using machine learning has shown that the connectivity profile between the salience and visual or anterior default mode can be used to predict age (La Corte et al., 2016). Healthy older individuals have reduced fronto-parietal and fronto-occiptial connectivity and lower regional clustering scores were correlated with diminished verbal and visual memory scores (Sala-Llonch et al., 2014). A study of working memory demonstrated healthy aged individuals had reduced default mode connectivity and that the degree of connectivity between the posterior cingulate cortex and medial prefrontal cortex correlated with memory performance (Sambataro et al., 2010). Human imaging studies have also noted a variety age-associated changes in network activation related to motor activity (Seidler et al., 2010) and learning (Mary et al., 2017). Our study found the greatest differences in connectivity and power to be in the somatomotor networks, therefore we focused our work to this region.

4.5. GCaMP imaging and aging

Group-level differences in neural activity and functional connectivity between young and old mice are likely a result of changes in patterns of intrinsic functional organization that naturally occur during normal aging, rather than as a result of changing GCaMP expression. Importantly, we did not find a significant difference in GCaMP positive cell count in aged animals, nor did we detect any of the characteristic signs of cellular stress or toxicity in this or our previous work (Rosenthal et al., 2020) (e.g. beading of axons, punctate expression of aggregated GCaMP, nuclear expression, or cellular atrophy). Additionally, stimulus-evoked responses were similar across aged and young animals, suggesting that the brain's ability to process sensory input was comparable across groups. Global reductions in signal power could result in reduced signal coherence, manifesting as lower values of zero-lag correlation. However, changes in FC were region specific while the very broad reductions in band-limited power involved the majority of the cortex. FC differences localized to select networks suggests that our measurements are sufficiently sensitive to detecting age-related alterations in functional brain organization processes.

4.6. Conclusions and limitations

The data presented here suggest that aging is associated with global declines in resting state activity across a wide range of frequencies and over large portions of the brain. In contrast, aging is associated with focal deterioration of cortical network connectivity most prominent in motor and somatosensory cortex. Finally, we report that whole-cortex delta band activity and node degree connectivity correlated with exploratory activity in young, but not aged mice. These data suggest that somatomotor network degradation driving diminished delta activity may disproportionally influence behavioral deficits with aging.

A limitation of our behavioral work is the correlative nature of our findings. While we see a clear correlation between delta frequency cortical network activity and exploratory behavior which is lost in the less active older animals, we can't discern if the lack of behavior drives the change in network activity or if the change in network activity drives the lack of behavior. Indeed, aged mice (by the time of the study) will have spent their entire lives in relatively small environments (standard cages). Alternatively, older mice may also be less interested in exploring unique environments having lived longer lives exposed to more things. The "novel" nature of the world to a younger animal may drive increased exploratory behavior. Future studies are needed to better differentiate the role of environment and long-term behavior patterns on network activity. Our study relies on mesoscale imaging of cortical network activity, therefore- we are limited in our ability to make assumptions about changes in subcortical activity and connectivity. Additionally, our study is primarily an examination of functional network activity. As discussed, a variety of synaptic and neuronal changes have been described with aging. An important part of future studies will be examining possible correlations between the network findings described here and structural changes in aged brains. Finally, while an advantage of our study is the broad frequency range we are able to examine using calcium imaging, we are still limited in our ability examine significantly faster cortical activity.

Supplementary Material

Refer to Web version on PubMed Central for supplementary material.

Acknowledgements

We thank Karen Smith for her help with behavior acquisition and animal care.

Funding

This work was supported by National Institute of Health grants R37NS110699 (JML), R01NS084028 (JML), R01NS094692 (JML), RO1-NS102870 (AQB), K25-NS083754 (AQB), R01NS078223 (JPC), P01NS080675 (JPC), F31NS103275 (ZPR), K08-NS109292-01A1 (ECL), as well as the McDonnell Center for Systems Neuroscience (AQB). This work was also supported by American Heart Association Grants 20CDA35310845 (AJA) and 20CDA35310607 (ECL).

References

Salthouse TA, 1998. Independence of age-related influences on cognitive abilities across the life span. Dev. Psychol 34, 851–864. [PubMed: 9779733]

Blazer DG, Yaffe K, Karlawish J, 2015. Cognitive aging: a report from the institute of medicine. JAMAJAMA 313, 2121–2122.

Shafto MA, Burke DM, Stamatakis EA, Tam PP, Tyler LK, 2007. On the tip-of-the–tongue: neural correlates of increased word-finding failures in normal aging. J. Cogn. Neurosci 19, 2060–2070. [PubMed: 17892392]

de Bruin N, Bryant DC, MacLean JN, Gonzalez CL, 2016. Assessing visuospatial abilities in healthy aging: a novel visuomotor task. Front Aging Neurosci. 8, 7. [PubMed: 26869918]

Bohannon RW, 1997. Comfortable and maximum walking speed of adults aged 20–79 years: reference values and determinants. Age Age. 26, 15–19.

Stockel T, Wunsch K, Hughes CML, 2017. Age-related decline in anticipatory motor planning and its relation to cognitive and motor skill proficiency. Front Aging Neurosci. 9, 283. [PubMed: 28928653]

Serrien DJ, Swinnen SP, Stelmach GE, 2000. Age-related deterioration of coordinated interlimb behavior. J. Gerontol. B Psychol. Sci. Soc. Sci 55, P295–P303. [PubMed: 10985294]

Terry RD, DeTeresa R, Hansen LA, 1987. Neocortical cell counts in normal human adult aging. Ann. Neurol 21, 530–539. [PubMed: 3606042]

Marner L, Nyengaard JR, Tang Y, Pakkenberg B, 2003. Marked loss of myelinated nerve fibers in the human brain with age. J. Comp. Neurol 462, 144–152. [PubMed: 12794739]

Salat DH, et al. , 2004. Thinning of the cerebral cortex in aging. Cereb. Cortex 14, 721–730. [PubMed: 15054051]

Morrison JH, Baxter MG, 2012. The ageing cortical synapse: hallmarks and implications for cognitive decline. Nat. Rev. Neurosci 13, 240–250. [PubMed: 22395804]

Dickstein DL, Weaver CM, Luebke JI, Hof PR, 2013. Dendritic spine changes associated with normal aging. Neurosci.Neurosci 251, 21–32.

Mostany R, et al. , 2013. Altered synaptic dynamics during normal brain aging. J. Neurosci 33, 4094–4104. [PubMed: 23447617]

Ou X, Buckwalter G, McNeill TH, Walsh JP, 1997. Age-related change in short-term synaptic plasticity intrinsic to excitatory striatal synapses. Synapse 27, 57–68. [PubMed: 9268065]

Shankar S, Teyler TJ, Robbins N, 1998. Aging differentially alters forms of long-term potentiation in rat hippocampal area CA1. J. Neurophysiol 79, 334–341. [PubMed: 9425202]

Yeatman JD, Wandell BA, Mezer AA, 2014. Lifespan maturation and degeneration of human brain white matter. Nat. Commun 5, 4932. [PubMed: 25230200]

Hasan KM, et al. , 2009. Diffusion tensor tractography quantification of the human corpus callosum fiber pathways across the lifespan. Brain Res. 1249, 91–100. [PubMed: 18996095]

Zhao T, et al. , 2015. Age-related changes in the topological organization of the white matter structural connectome across the human lifespan. Hum. Brain Mapp 36, 3777–3792. [PubMed: 26173024]

Giraud AL, Poeppel D, 2012. Cortical oscillations and speech processing: emerging computational principles and operations. Nat. Neurosci 15, 511–517. [PubMed: 22426255]

Ward LM, 2003. Synchronous neural oscillations and cognitive processes. Trends Cogn. Sci 7, 553–559. [PubMed: 14643372]

Klimesch W, 1999. EEG alpha and theta oscillations reflect cognitive and memory performance: a review and analysis. Brain Res. Brain Res. Rev 29, 169–195. [PubMed: 10209231]

Vlahou EL, Thurm F, Kolassa IT, Schlee W, 2014. Resting-state slow wave power, healthy aging and cognitive performance. Sci. Rep 4, 5101. [PubMed: 24869503]

Damoiseaux JS, 2017. Effects of aging on functional and structural brain connectivity. NeuroimageNeuroi. 160, 32–40.

Wu JT, et al. , 2011. Aging-related changes in the default mode network and its anti-correlated networks: a resting-state fMRI study. Neurosci. Lett 504, 62–67. [PubMed: 21925236]

Grady C, Sarraf S, Saverino C, Campbell K, 2016. Age differences in the functional interactions among the default, frontoparietal control, and dorsal attention networks. Neurobiol. Aging 41, 159–172. [PubMed: 27103529]

Yoshimura N, et al. , 2020. Age-related decline of sensorimotor integration influences resting-state functional brain connectivity. Brain Sci. 10.

Mary A, et al. , 2017. Resting-state functional connectivity is an age-dependent predictor of motor learning abilities. Cereb. Cortex 27, 4923–4932. [PubMed: 27655931]

Sala-Llonch R, et al. , 2014. Changes in whole-brain functional networks and memory performance in aging. Neurobiol. Aging 35, 2193–2202. [PubMed: 24814675]

Burle B, et al. , 2015. Spatial and temporal resolutions of EEG: is it really black and white? A scalp current density view. Int. J. Psychophysiol 97, 210–220. [PubMed: 25979156]

Srinivasan R, Nunez PL, Tucker DM, Silberstein RB, Cadusch PJ, 1996. Spatial sampling and filtering of EEG with spline laplacians to estimate cortical potentials. Brain Topogr. 8, 355–366. [PubMed: 8813415]

McCann H, Pisano G, Beltrachini L, 2019. Variation in reported human head tissue electrical conductivity values. Brain Topogr. 32, 825–858. [PubMed: 31054104]

Anderson JS, 2008. Origin of synchronized low-frequency blood oxygen level-dependent fluctuations in the primary visual cortex. AJNR Am. J. Neuroradiol 29, 1722–1729. [PubMed: 18635612]

Logothetis NK, Wandell BA, 2004. Interpreting the BOLD signal. Annu. Rev. Physiol 66, 735–769. [PubMed: 14977420]

Fabiani M, et al. , 2014. Neurovascular coupling in normal aging: a combined optical, ERP and fMRI study. NeuroimageNeuroi. 85 Pt 1, 592–607.

Park L, Anrather J, Girouard H, Zhou P, Iadecola C, 2007. Nox2-derived reactive oxygen species mediate neurovascular dysregulation in the aging mouse brain. J. Cereb. Blood Flow Metab 27, 1908–1918. [PubMed: 17429347]

Chen Q, et al. , 2012. Imaging neural activity using Thy1-GCaMP transgenic mice. NeuronNeuron 76, 297–308.

Dana H, et al. , 2014. Thy1-GCaMP6 transgenic mice for neuronal population imaging in vivo. PLoS ONE 9, e108697. [PubMed: 25250714]

Xiao D, et al. , 2017. Mapping cortical mesoscopic networks of single spiking cortical or sub-cortical neurons. Elife 6.

Brier LM, et al. , 2019. Separability of calcium slow waves and functional connectivity during wake, sleep, and anesthesia. Neurophotonics 6, 035002. [PubMed: 31930154]

Wright PW, et al. , 2017. Functional connectivity structure of cortical calcium dynamics in anesthetized and awake mice. PLoS ONE 12, e0185759. [PubMed: 29049297]

Fox JG, 2007. ScienceDirect, The Mouse in Biomedical research, American College of Laboratory Animal Medicine series. Academic Press, Amsterdam; New York 2nd upd. and rev..

Studenski S, et al. , 2011. Gait speed and survival in older adults. JAMAJAMA 305, 50–58.

Rosenthal ZP, et al. , 2020. Local perturbations of cortical excitability propagate differentially through large-scale functional networks. Cereb. Cortex 30, 3352–3369. [PubMed: 32043145]

Kraft AW, Bauer AQ, Culver JP, Lee JM, 2018. Sensory deprivation after focal ischemia in mice accelerates brain remapping and improves functional recovery through Arc-dependent synaptic plasticity. Sci. Transl. Med 10.

White BR, et al. , 2011. Imaging of functional connectivity in the mouse brain. PLoS ONE 6, e16322. [PubMed: 21283729]

Franklin KBJ, Paxinos G, 2013. Paxinos and Franklin's The Mouse Brain in Stereotaxic Coordinates. Academic Press, an imprint of Elsevier, Amsterdam, p. 1 ed. Fourth edition.volume (unpaged).

Bauer AQ, et al. , 2014. Optical imaging of disrupted functional connectivity following ischemic stroke in mice. NeuroimageNeuroi. 99, 388–401.

Bero AW, et al. , 2012. Bidirectional relationship between functional connectivity and amyloid-beta deposition in mouse brain. J. Neurosci 32, 4334–4340. [PubMed: 22457485]

Hakon J, et al. , 2018. Multisensory stimulation improves functional recovery and resting-state functional connectivity in the mouse brain after stroke. Neuroimage Clin. 17, 717–730. [PubMed: 29264113]

Maris E, Oostenveld R, 2007. Nonparametric statistical testing of EEG- and MEG-data. J. Neurosci. Methods 164, 177–190. [PubMed: 17517438]

Lu H, Jaime S, Yang Y, 2019. Origins of the resting-state functional MRI signal: potential limitations of the "Neurocentric" model. Front Neurosci. 13, 1136. [PubMed: 31708731]

Lamberty Y, Gower AJ, 1992. Age-related changes in spontaneous behavior and learning in NMRI mice from middle to old age. Physiol. Behav 51, 81–88. [PubMed: 1741453]

Milanovic Z, et al. , 2013. Age-related decrease in physical activity and functional fitness among elderly men and women. Clin. Interv. Aging 8, 549–556. [PubMed: 23723694]

Schallert T, Fleming SM, Leasure JL, Tillerson JL, Bland ST, 2000. CNS plasticity and assessment of forelimb sensorimotor outcome in unilateral rat models of stroke, cortical ablation, parkinsonism and spinal cord injury. Neuropharmacology-Neuropharmacol. 39, 777–787.

Buzsaki G, Draguhn A, 2004. Neuronal oscillations in cortical networks. ScienceSci. 304, 1926–1929.

Cebolla AM, Cheron G, 2019. Understanding neural oscillations in the human brain: from movement to consciousness and vice versa. Front Psychol. 10, 1930. [PubMed: 31507490]

Varela F, Lachaux JP, Rodriguez E, Martinerie J, 2001. The brainweb: phase synchronization and large-scale integration. Nat. Rev. Neurosci 2, 229–239. [PubMed: 11283746]

O'Sullivan M, et al. , 2001. Evidence for cortical "disconnection" as a mechanism of age-related cognitive decline. NeurologyNeurol. 57, 632–638.

Varangis E, Habeck CG, Razlighi QR, Stern Y, 2019. The Effect of Aging on Resting State Connectivity of Predefined Networks in the Brain. Front Aging Neurosci. 11, 234. [PubMed: 31555124]

Grady C, 2012. The cognitive neuroscience of ageing. Nat. Rev. Neurosci 13, 491–505. [PubMed: 22714020]

Andrews-Hanna JR, et al. , 2007. Disruption of large-scale brain systems in advanced aging. NeuronNeuron 56, 924–935.

Avelar-Pereira B, Backman L, Wahlin A, Nyberg L, Salami A, 2017. Age-related differences in dynamic interactions among default mode, frontoparietal control, and dorsal attention networks during resting-state and interference resolution. Front Aging Neurosci. 9, 152. [PubMed: 28588476]

Campbell KL, Grady CL, Ng C, Hasher L, 2012. Age differences in the frontoparietal cognitive control network: implications for distractibility. NeuropsychologiaNeuropsychol. 50, 2212–2223.

Bo J, et al. , 2014. Lifespan differences in cortico-striatal resting state connectivity. Brain Connect. 4, 166–180. [PubMed: 24575740]

Egimendia A, et al. , 2019. Aging reduces the functional brain networks strength-a resting state fMRI study of healthy mouse brain. Front Aging Neurosci. 11, 277. [PubMed: 31680932]

Barnes CA, McNaughton BL, O'Keefe J, 1983. Loss of place specificity in hippocampal complex spike cells of senescent rat. Neurobiol. Aging 4, 113–119. [PubMed: 6633780]

Grady CL, et al. , 1994. Age-related changes in cortical blood flow activation during visual processing of faces and location. J. Neurosci 14, 1450–1462. [PubMed: 8126548]

Park DC, et al. , 2004. Aging reduces neural specialization in ventral visual cortex. Proc. Natl. Acad. Sci. U. S. A 101, 13091–13095. [PubMed: 15322270]

Logan JM, Sanders AL, Snyder AZ, Morris JC, Buckner RL, 2002. Under-recruitment and nonselective recruitment: dissociable neural mechanisms associated with aging. NeuronNeuron 33, 827–840.

Chan MY, Park DC, Savalia NK, Petersen SE, Wig GS, 2014. Decreased segregation of brain systems across the healthy adult lifespan. Proc. Natl. Acad. Sci. U. S. A 111, E4997–E5006. [PubMed: 25368199]

Fox MD, et al. , 2005. The human brain is intrinsically organized into dynamic, anticorrelated functional networks. Proc. Natl. Acad. Sci. U. S. A 102, 9673–9678. [PubMed: 15976020]

Spreng RN, Stevens WD, Viviano JD, Schacter DL, 2016. Attenuated anticorrelation between the default and dorsal attention networks with aging: evidence from task and rest. Neurobiol. Aging 45, 149–160. [PubMed: 27459935]

Mitra A, et al. , 2018. Spontaneous infra-slow brain activity has unique spatiotemporal dynamics and laminar structure. NeuronNeuron 98, 297–305 e296.

Scher MS, 2008. Ontogeny of EEG-sleep from neonatal through infancy periods. Sleep Med. 9, 615–636. [PubMed: 18024172]

Dijk DJ, 2009. Regulation and functional correlates of slow wave sleep. J Clin Sleep Med 5, S6–15. [PubMed: 19998869]

Knyazev GG, 2012. EEG delta oscillations as a correlate of basic homeostatic and motivational processes. Neurosci. Biobehav. Rev 36, 677–695. [PubMed: 22020231]

Knyazev GG, 2007. Motivation, emotion, and their inhibitory control mirrored in brain oscillations. Neurosci. Biobehav. Rev 31, 377–395. [PubMed: 17145079]

Lakatos P, Karmos G, Mehta AD, Ulbert I, Schroeder CE, 2008. Entrainment of neuronal oscillations as a mechanism of attentional selection. ScienceScience 320, 110–113.

Hoffman LD, Polich J, 1998. EEG, ERPs and food consumption. Biol. Psychol 48, 139–151. [PubMed: 9700015]

Savory CJ, Kostal L, 2006. Is expression of some behaviours associated with de-arousal in restricted-fed chickens? Physiol. Behav 88, 473–478. [PubMed: 16806324]

Reid MS, et al. , 2003. Quantitative electroencephalographic studies of cue-induced cocaine craving. Clin. Electroencephalogr 34, 110–123. [PubMed: 14521273]

Bernard C, et al. , 2015. PCC characteristics at rest in 10-year memory decliners. Neurobiol. Aging 36, 2812–2820. [PubMed: 26234756]

Onoda K, Ishihara M, Yamaguchi S, 2012. Decreased functional connectivity by aging is associated with cognitive decline. J. Cogn. Neurosci 24, 2186–2198. [PubMed: 22784277]

La Corte V, et al. , 2016. Cognitive decline and reorganization of functional connectivity in healthy aging: the pivotal role of the salience network in the prediction of age and cognitive performances. Front Aging Neurosci. 8, 204. [PubMed: 27616991]

Sambataro F, et al. , 2010. Age-related alterations in default mode network: impact on working memory performance. Neurobiol. Aging 31, 839–852. [PubMed: 18674847]

Seidler RD, et al. , 2010. Motor control and aging: links to age-related brain structural, functional, and biochemical effects. Neurosci. Biobehav. Rev 34, 721–733. [PubMed: 19850077]

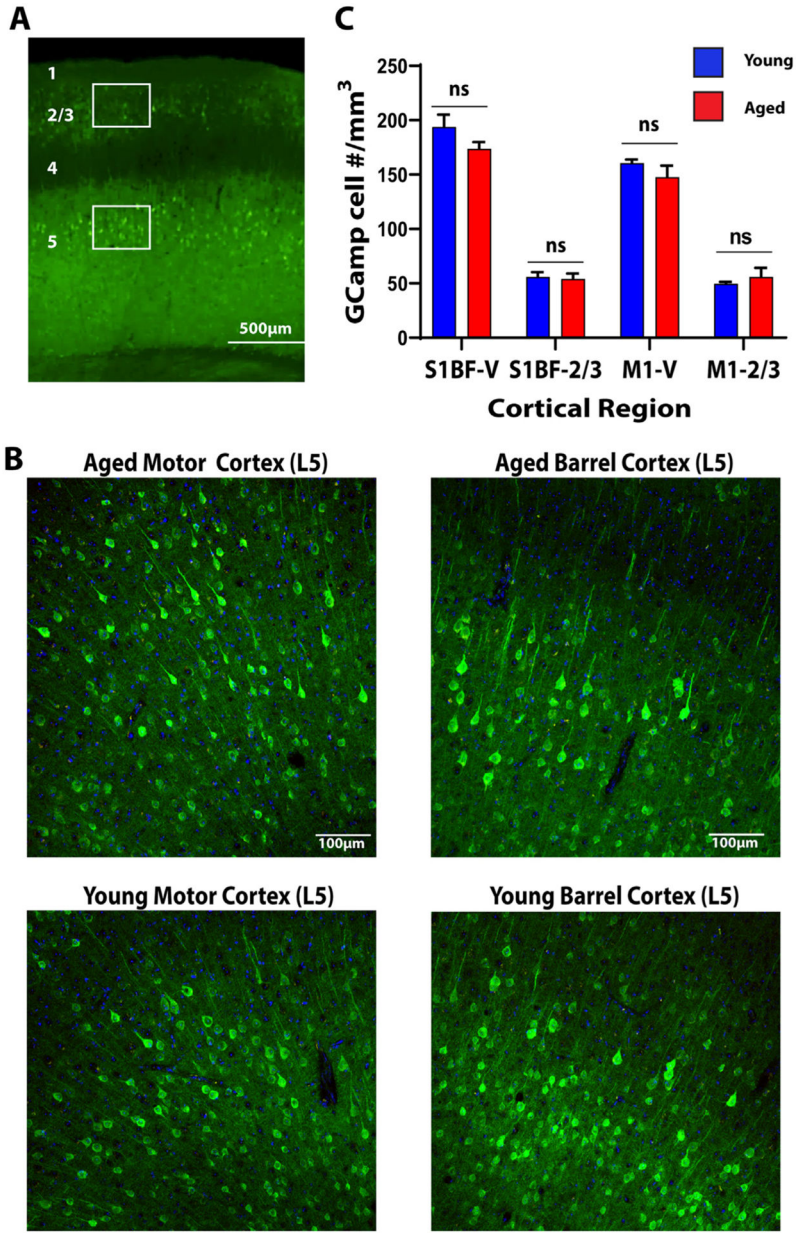

Fig. 1. Young and Aged Mice have Similar Cortical GCaMP Expression.

A. Low magnification view of the cortex. Numbers represent cortical layers. Boxes represent regions of interest in which counts were undertaken. **B.** Representative expression patterns from layer 5 motor and barrel cortex in aged and young animals. **C.** Quantification of GCaMP positive cell count in Layer 2/3 and Layer 5 barrel and motor cortices in aged (red) vs young (blue) animals.

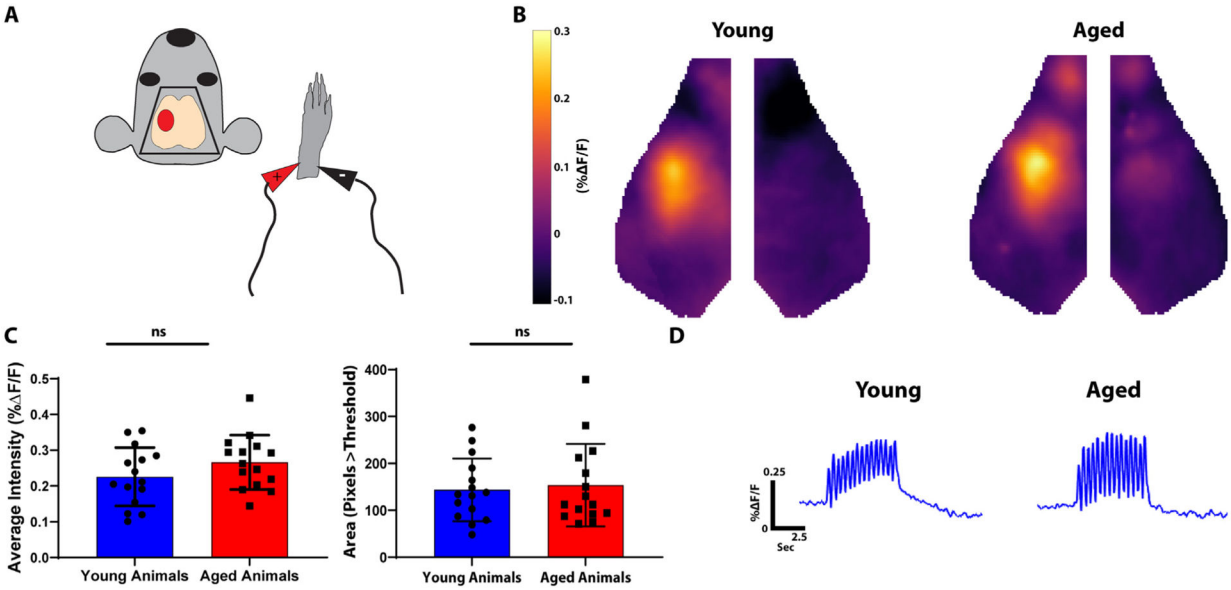

Fig. 2. Young and Aged Mice have Similar Patterns of Evoked Somatosensory Cortex Activity.

A. Diagram of experimental paradigm. The right forepaw was stimulated with mild electrical pulsations and contralateral somatosensory cortex activity was imaged (red oval). **B.** Average somatosensory activation in young (left) and aged (right) animals. **C.** Quantification of evoked somatosensory activity. The left graph represents average intensity within a somatosensory ROI. The right graph represents total area of activation as measured by pixels greater than threshold. **D.** Averaged fluorescence amplitude curves over time within a somatosensory ROI in young (left) vs. aged (right) animals.

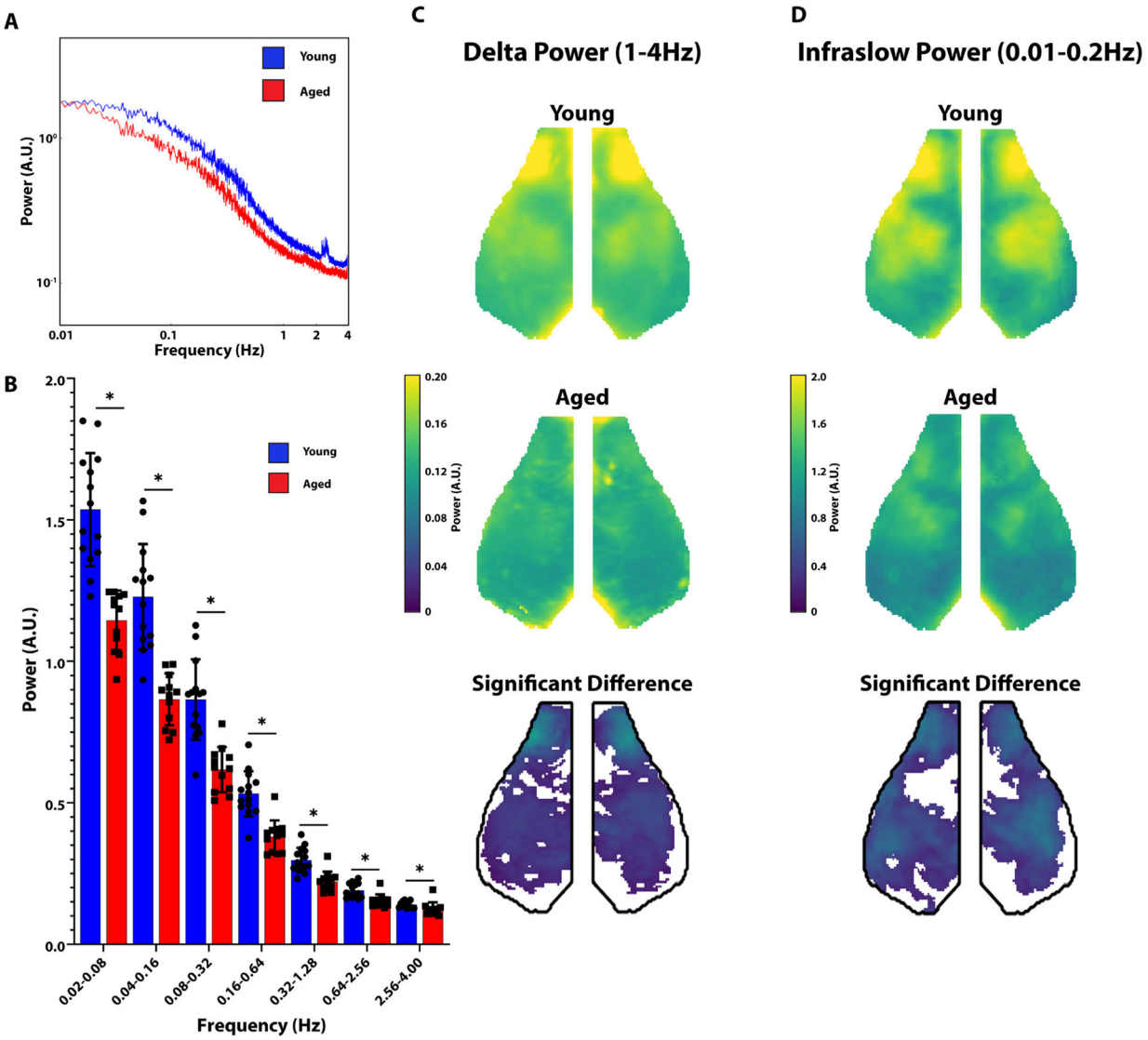

Fig. 3. Aged Animals have Significantly Reduced Resting State Power.

A. Power spectral density is shown in arbitrary units (A.U.). Graph of Power as a function of frequency in aged (red) vs young (blue) animals. **B.** Whole-cortex power divided into octaves in young (blue) vs. aged (red) animals. Young animals had significantly greater whole-cortex power at all measured frequencies. **C.** Group averaged maps of whole-cortex delta (left) power in young animals (top row) and aged animals (middle row). The bottom row represents the difference between young and aged groups (young-aged) thresholded for significance. **D.** Same as C but in the infraslow band.

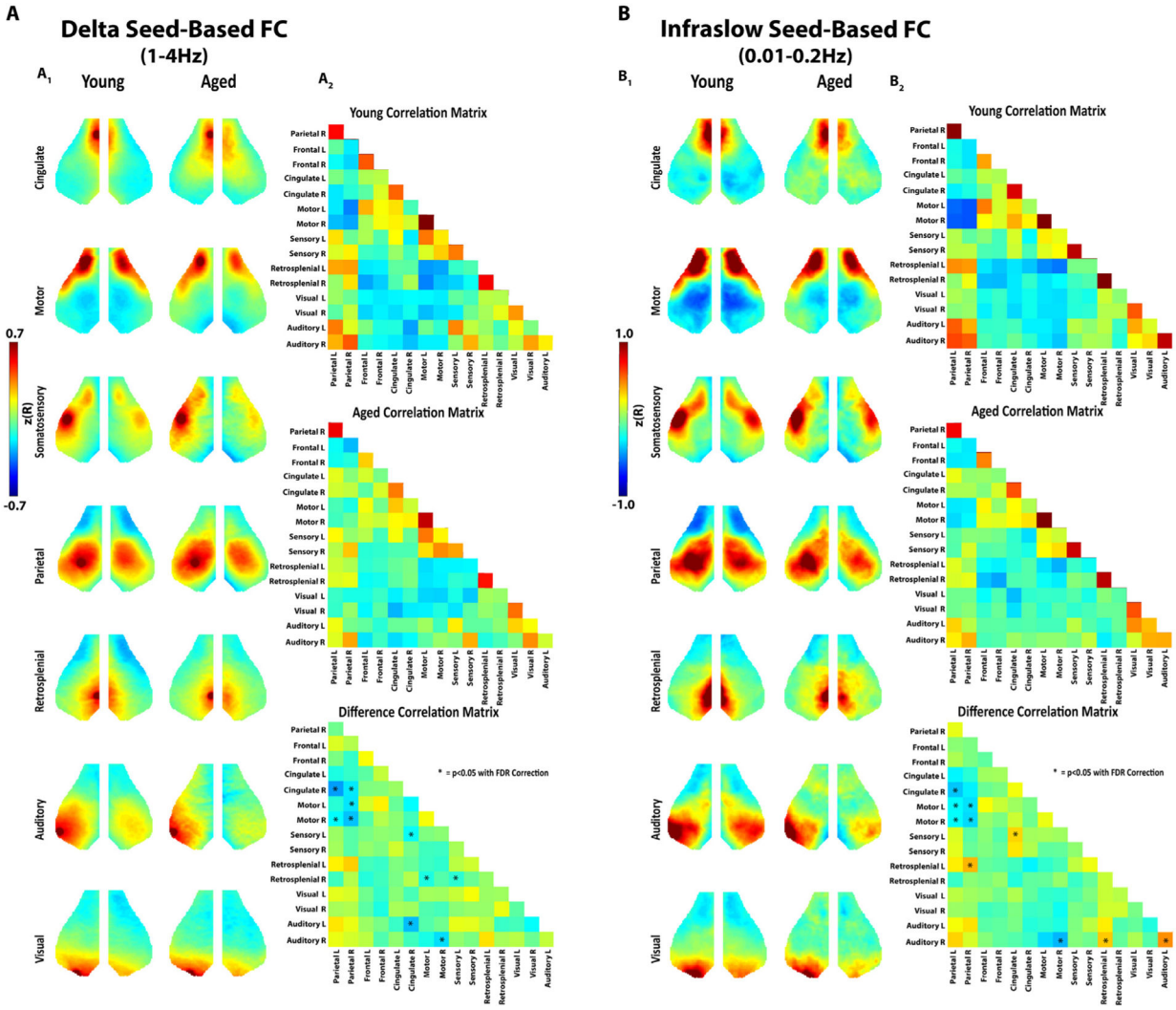

Fig. 4. Aged Animals have Significantly Reduced Internetwork Connectivity using Seed Based Analysis

A_1. Seed based analysis of functionally connected networks in the mouse cortex in the delta frequency band. Each map represents group average connectivity values for seeds placed in distinct regions (as labeled). The left column is young animals. The right column is older animals. **A_2**. Connectivity correlation matrices for all seeds in young animals (top), aged animals (middle), and the difference between the two (young minus aged) (bottom). Asterisks are placed over cells in the matrix that represent a significant difference ($p<0.05$ with FDR correction). **B_1**. Seed based analysis of functionally connected networks in the mouse cortex in the infraslow frequency band. Group average maps are shown similar to A. **B_2**. Correlation matrices in the infraslow band similar to A.

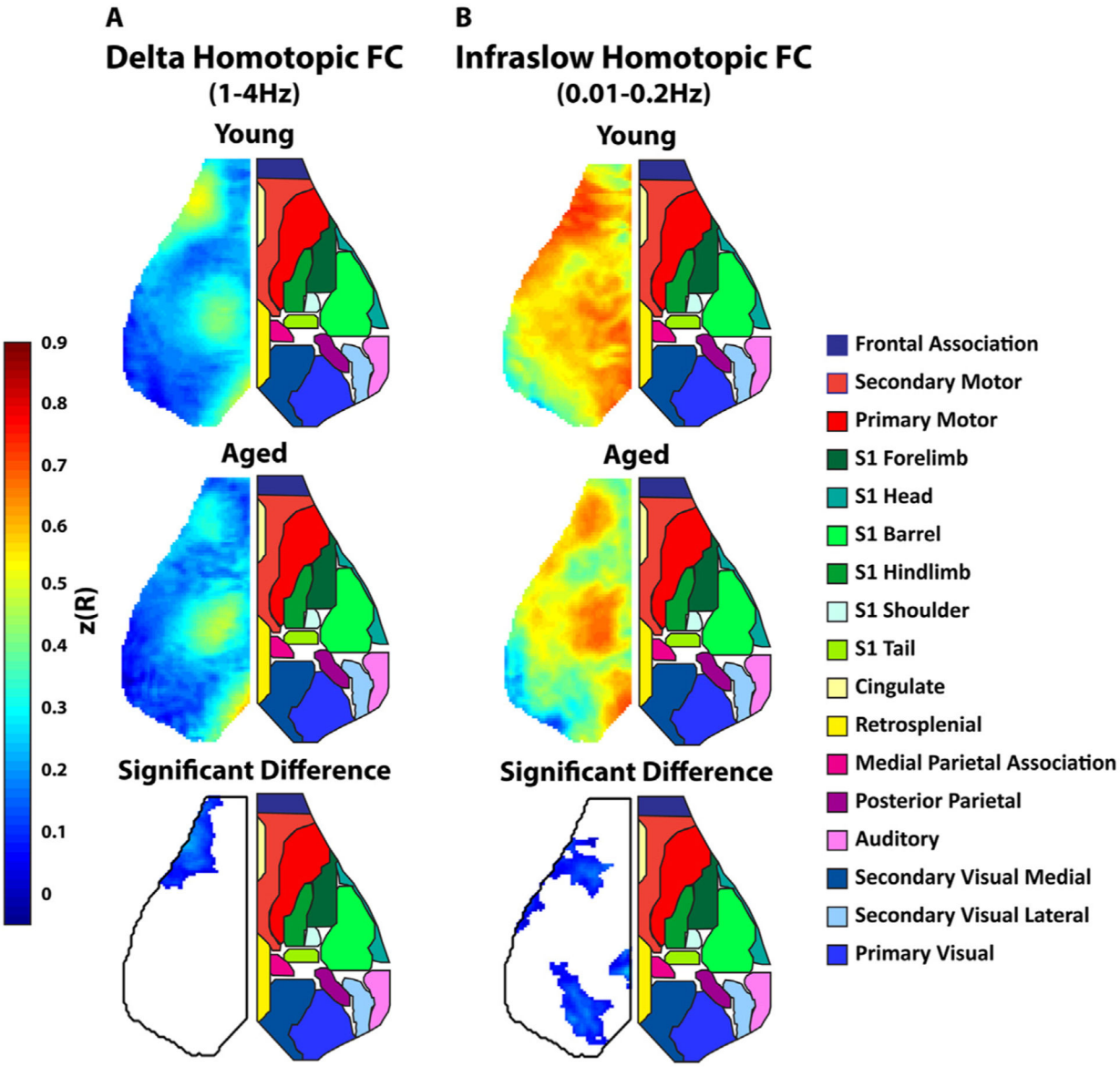

Fig. 5. Aged Animals have Significantly Reduced Homotopic Functional Connectivity

A. Group averaged maps of whole-cortex homotopic FC (correlation between each pixel and its mirror pixel) in the delta (1–4 Hz) frequency band. Top map is the average homotopic FC in young animals. The middle map is average homotopic FC in aged animals. The bottom map is difference between the average young and aged maps (young-aged) thresholded for significance. Since the maps were symmetric, the left side of the cortex is shown and the right side shows a map of approximate cortical networks based on the Paxinos atlas. **B.** Similar group average maps as **A** but in the infraslow band.

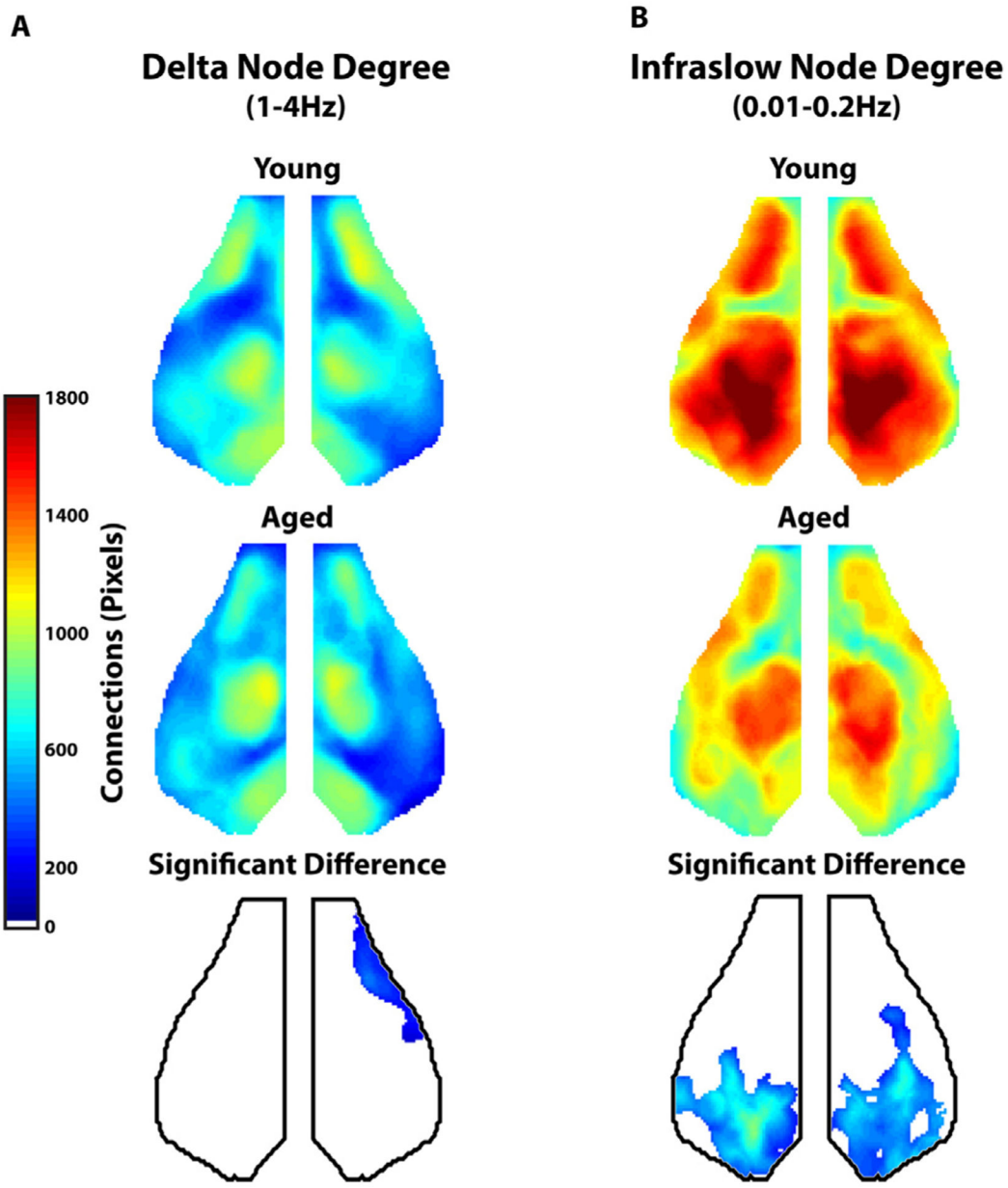

Fig. 6. Aged Animals Have Significant Reduction in Global Node Degree

A. Group average map of global (whole cortex) node degree in the delta frequency range (1–4 Hz) for young (top) and aged (middle) animals. The bottom map represents the difference between young and aged animals in global node degree thresholded for significance. **B.** Group average map of global (whole cortex) node degree in the infraslow frequency range (0.01–0.2 Hz) for young (top) and aged (middle) animals. The bottom map represents the difference between young and aged animals in global node degree thresholded for significance.

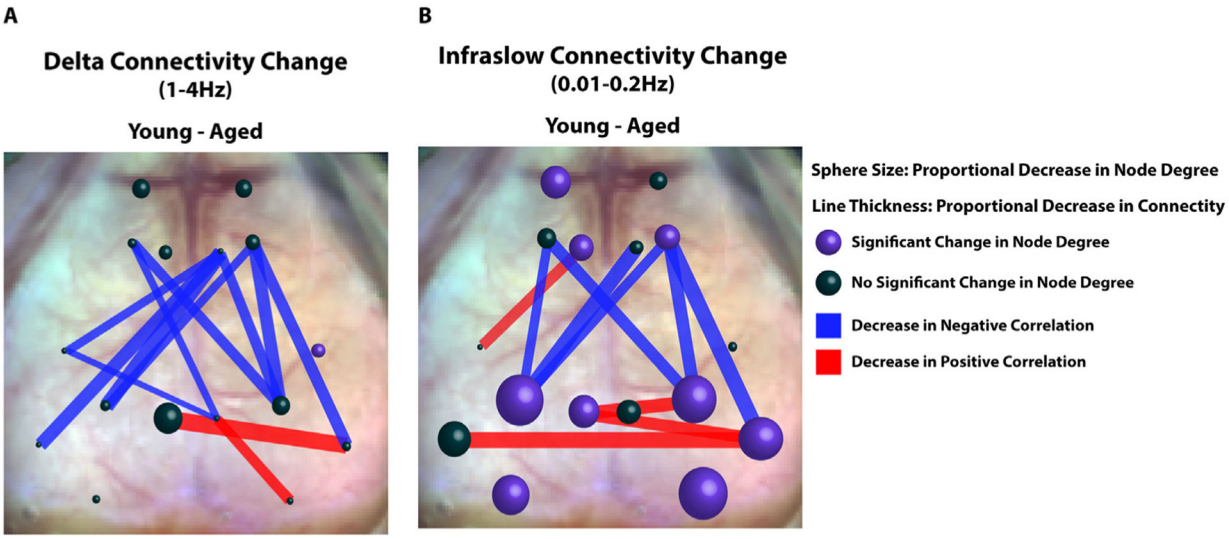

Fig. 7. Summary of Connectivity Changes in Aged vs. Young Animals

A. Representative diagram of connectivity difference between young and aged animals (young minus aged) within the delta band. Spheres are at locations of seeds used in seed-based FC analysis. Sphere size correlates to the average change in node degree within the seed between young and aged mice (Young - Aged). Average node degree within the seeds was compared between young and aged animals using a student's T test. Purple spheres represent significant differences in average node degree at that location ($p<0.05$). Lines between seeds represent significant differences in connectivity (z(R)) between young and aged groups. The thickness of the lines is proportional to magnitude of the correlation difference. Red lines represent age associated decreases in positive correlations and blue lines represent age-associated decreases in negative correlations. **B** Same as A, but in the infraslow band.

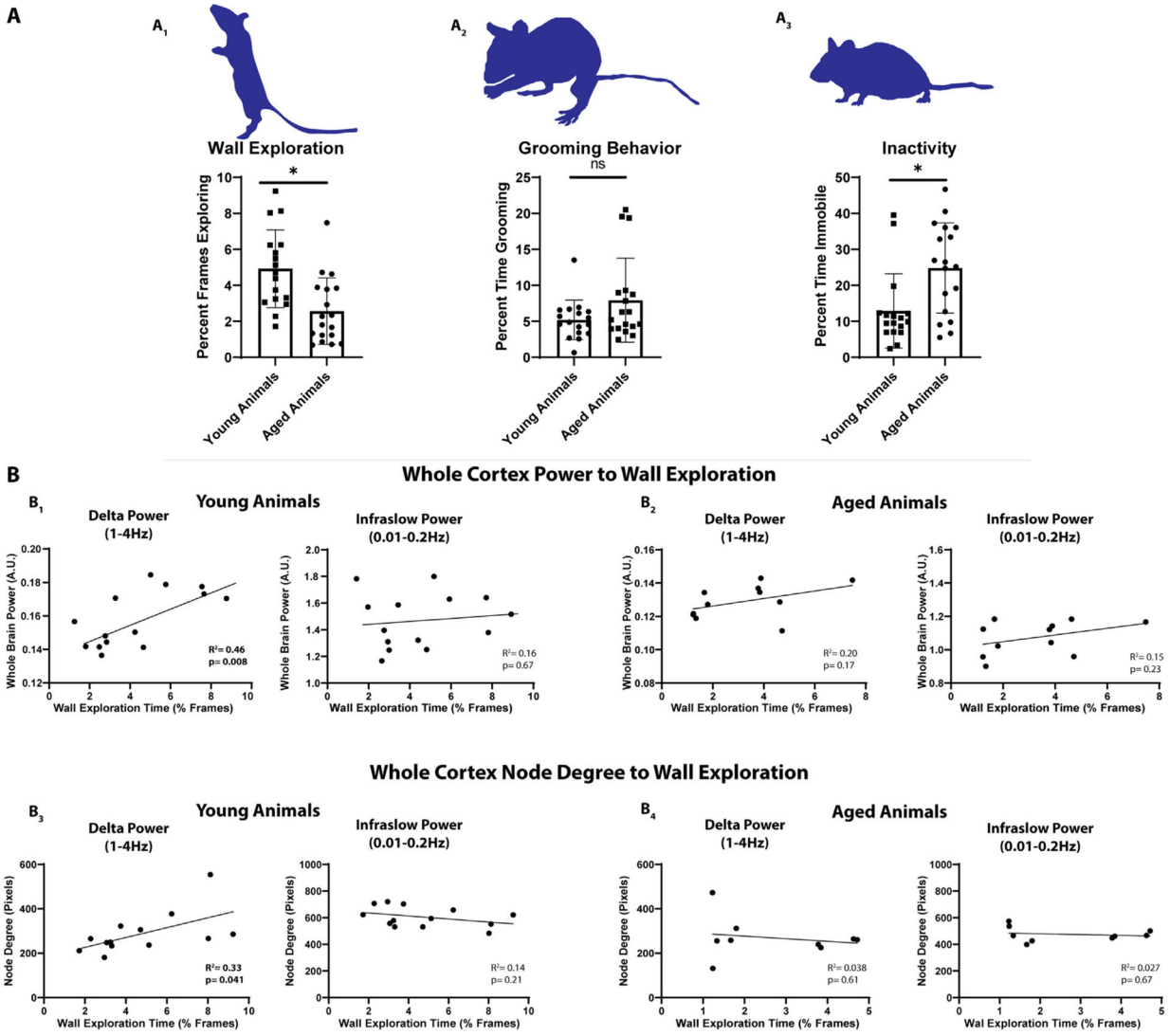

Fig. 8. Exploratory Behavior in Young Animals Correlates with Cortical Delta Power and Delta Node Degree

A_1. Young animals (n = 17) explored a clear glass container significantly more than aged animals (n = 18). **A_2**. Grooming behavior was similar in aged and young animals. **A_3**. Aged animals spent significantly more time immobile than young animals. **B_1**. Whole-cortex power significantly correlated with the degree of wall exploration observed in young animals (n = 14) within the delta but not infraslow frequency band. **B_2**. Whole-cortex power in aged animals (n = 11) did not correlate with exploration time in either the delta or infraslow frequency band. **B_3**. Whole-cortex node degree correlated significantly (R^2=0.43) with the degree of wall exploration within the delta but not infraslow frequency band in young animals (n = 13). Infraslow node degree did not correlate. **B_4**. There was no correlation between delta or infraslow node degree and exploration in aged animals (n = 9).